Supplementary Information

Supplementary Figures

Supplementary Tables

Supplementary Material and methods

Supplementary References

Figure S1

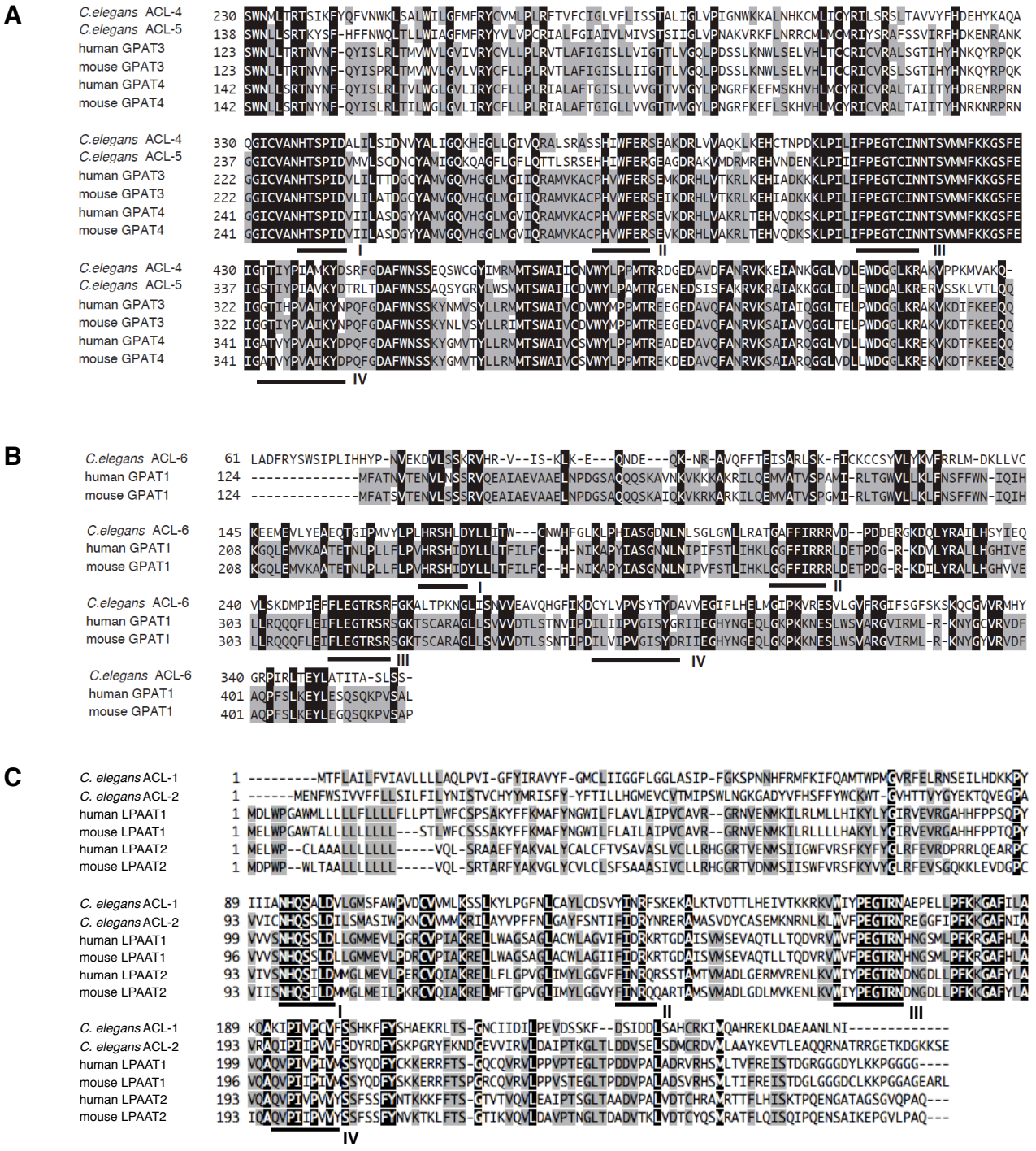
A
C.elegans ACL-4
C.elegans ACL-5
human GPAT3
mouse GPAT3
human GPAT4
mouse GPAT4
I
II
III
IV
B
C.elegans ACL-6
human GPAT1
mouse GPAT1
I
II
III
IV
C
C. elegans ACL-1
C. elegans ACL-2
human LPAAT1
mouse LPAAT1
human LPAAT2
mouse LPAAT2
I
II
III
IV

Figure S2

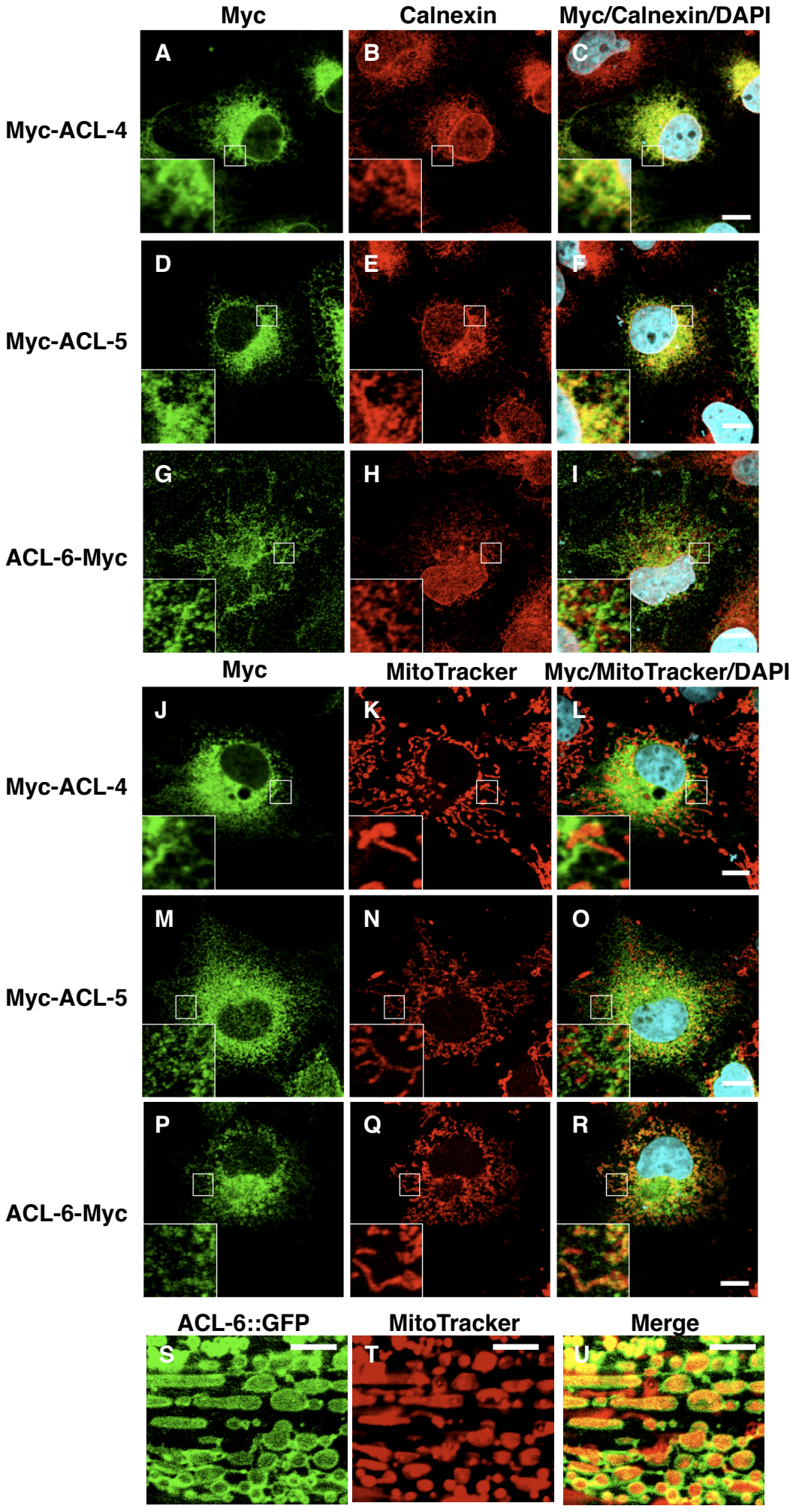
Myc
Calnexin
Myc/Calnexin/DAPI
Myc-ACL-4
Myc-ACL-5
ACL-6-Myc
A
B
C
D
E
F
G
H
I
Myc
MitoTracker
Myc/MitoTracker/DAPI
Myc-ACL-4
Myc-ACL-5
ACL-6-Myc
J
K
L
M
N
O
P
Q
R
ACL-6::GFP
MitoTracker
Merge
S
T
U

Figure S3

A Wild-type (*ccIs4251*)

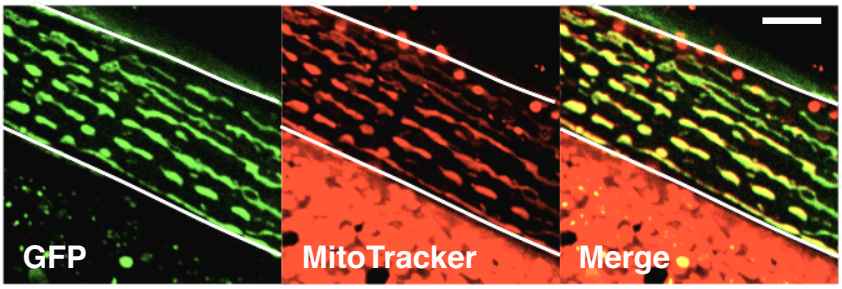

B Mt-GPAT (*acl-6*) mutant (*acl-6; ccIs4251*)

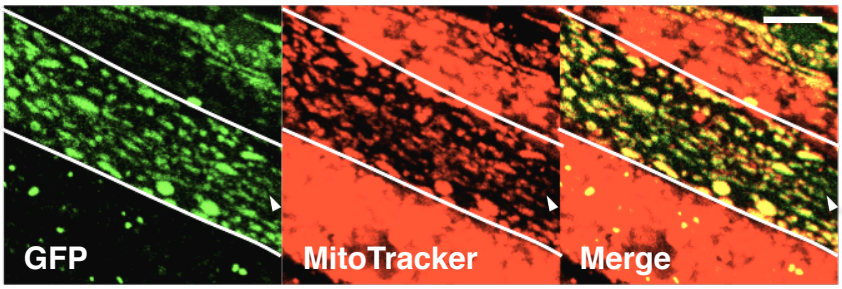

Figure S4

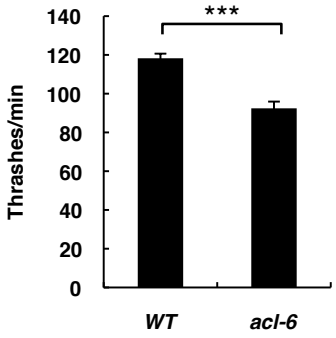

Figure S5

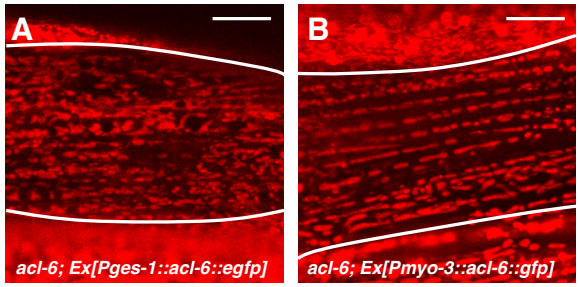
A
acl-6; Ex[Pges-1::acl-6::egfp]
B
acl-6; Ex[Pmyo-3::acl-6::gfp]

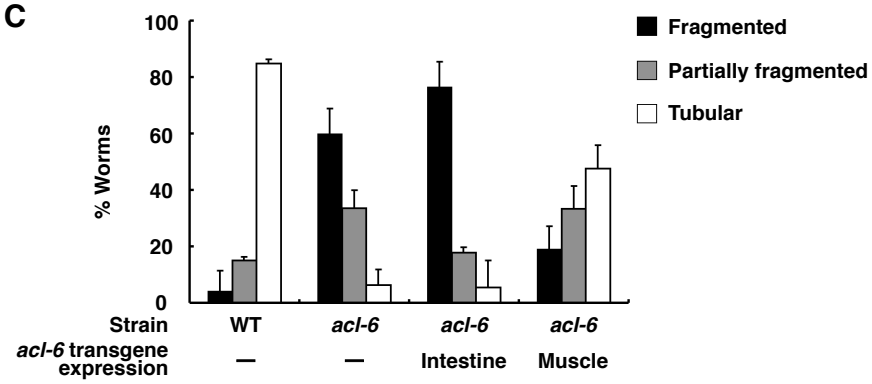
C
% Worms
100
80
60
40
20
0
Fragmented
Partially fragmented
Tubular
Strain
WT
acl-6
acl-6
acl-6
acl-6 transgene expression
—
—
Intestine
Muscle

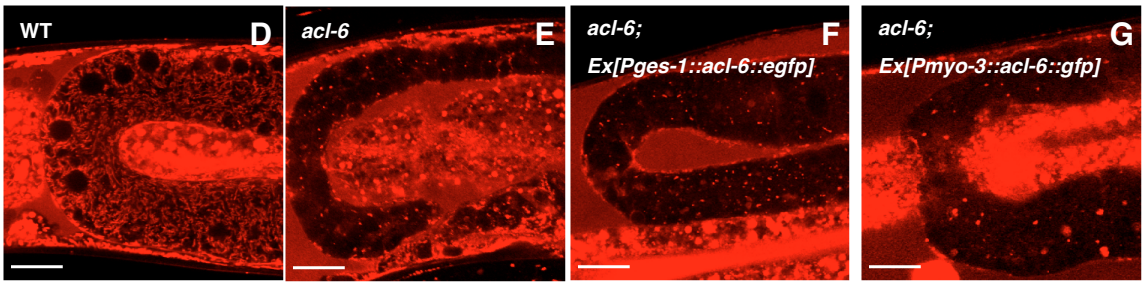
WT
D
acl-6
E
acl-6;
Ex[Pges-1::acl-6::egfp]
F
acl-6;
Ex[Pmyo-3::acl-6::gfp]
G

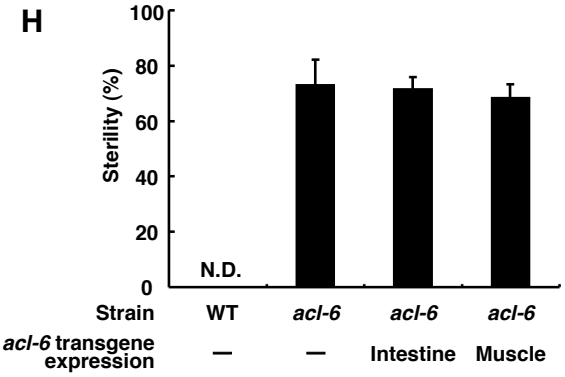
H
Sterility (%)
100
80
60
40
20
0
N.D.
Strain
WT
acl-6
acl-6
acl-6
acl-6 transgene expression
—
—
Intestine
Muscle

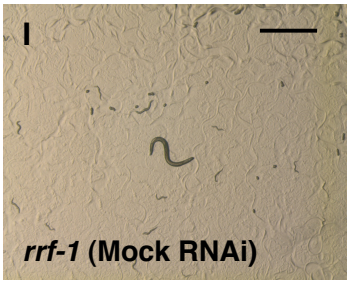
I
rrf-1 (Mock RNAi)

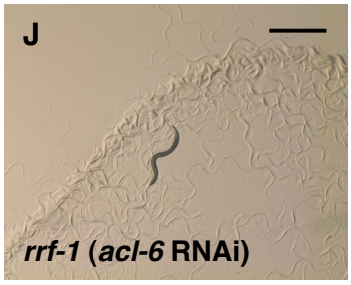
J
rrf-1 (acl-6 RNAi)

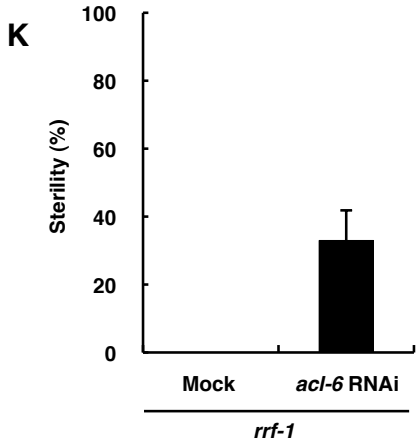
K
Sterility (%)
100
80
60
40
20
0
Mock
acl-6 RNAi
rrf-1

Figure S6

A

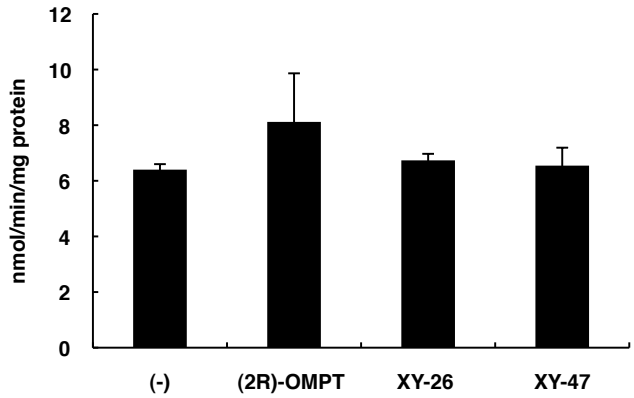

B

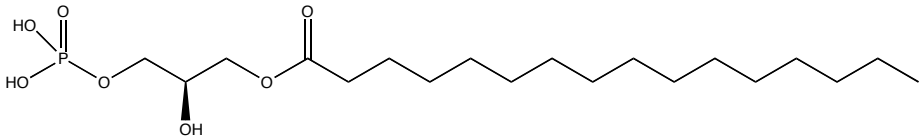

C

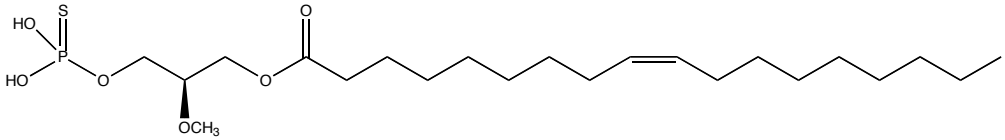

D

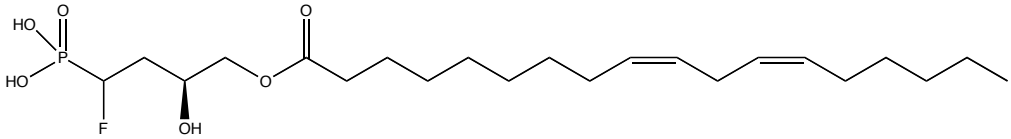

E

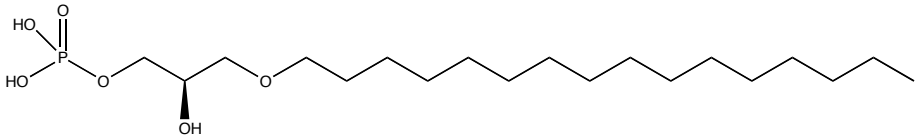

Figure S7

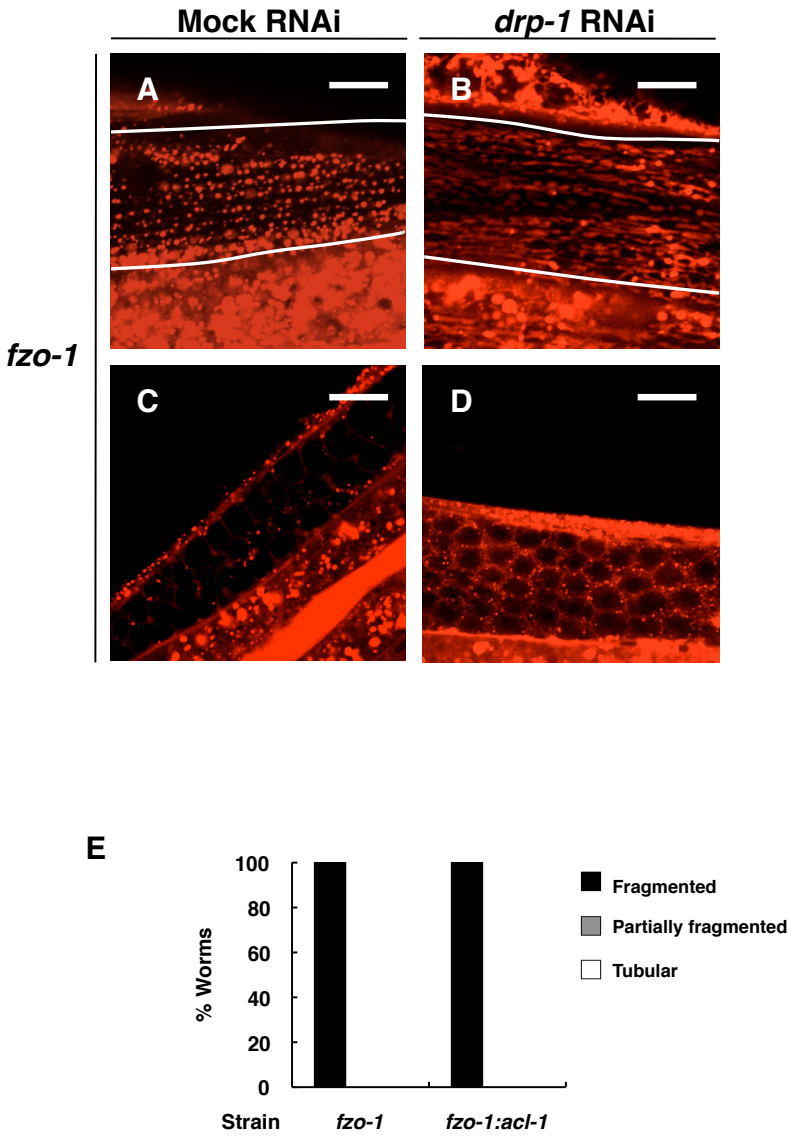
Mock RNAi
drp-1 RNAi
fzo-1
A
B
C
D
E
100
80
60
40
20
0
% Worms
Strain
fzo-1
fzo-1:acl-1
Fragmented
Partially fragmented
Tubular

Figure S8

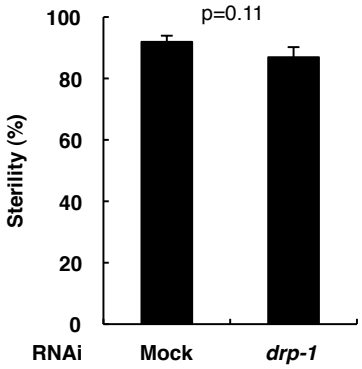

Figure S9

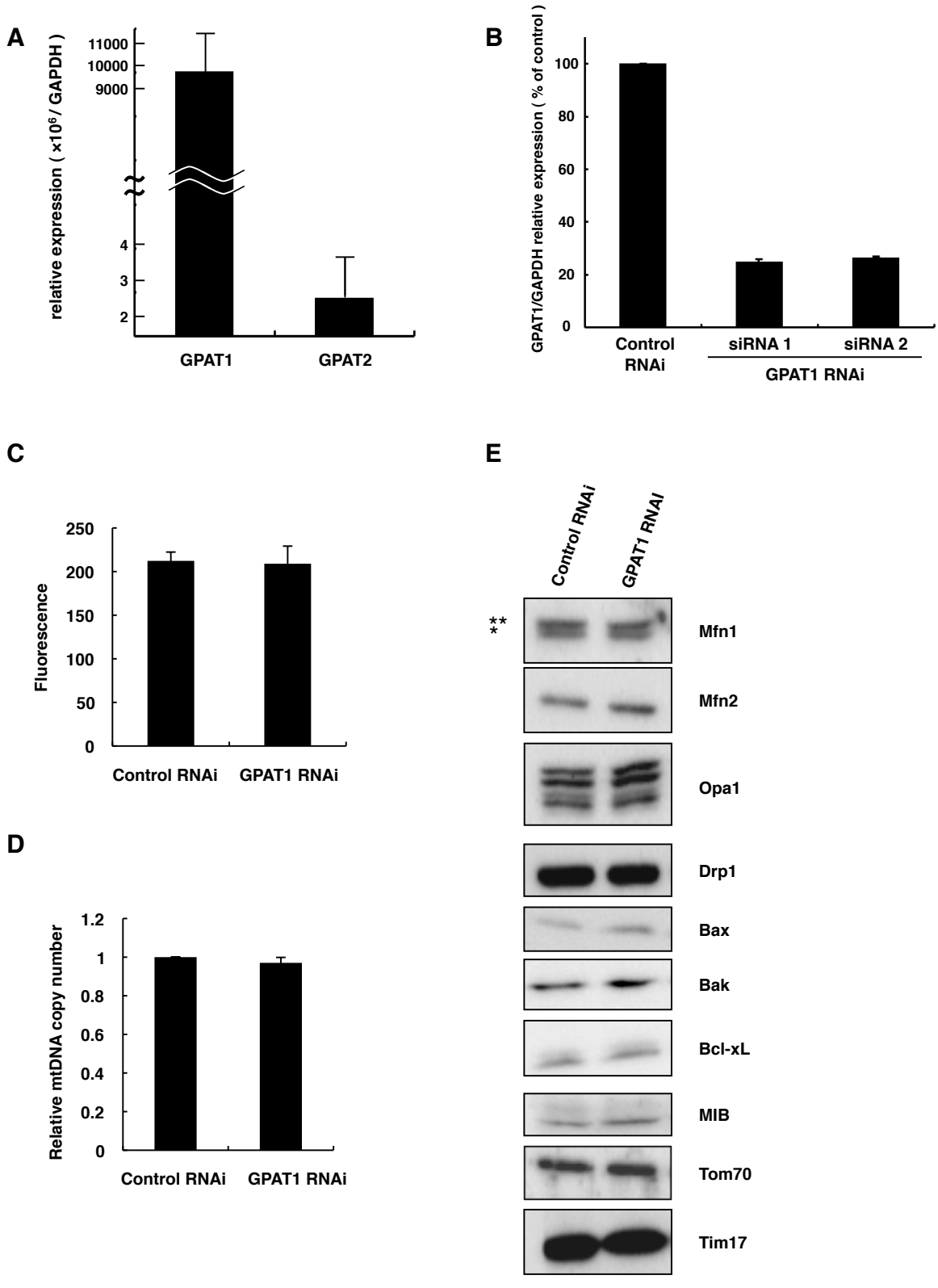
A
relative expression (×10⁶/ GAPDH)
11000
10000
9000
4
3
2
GPAT1
GPAT2
B
GPAT1/GAPDH relative expression (% of control)
100
80
60
40
20
0
Control RNAi
siRNA 1
siRNA 2
GPAT1 RNAi
C
Fluorescence
250
200
150
100
50
0
Control RNAi
GPAT1 RNAi
D
Relative mtDNA copy number
1.2
1
0.8
0.6
0.4
0.2
0
Control RNAi
GPAT1 RNAi
E
Control RNAi
GPAT1 RNAi
**
Mfn1
Mfn2
Opa1
Drp1
Bax
Bak
Bcl-xL
MIB
Tom70
Tim17

Figure S10

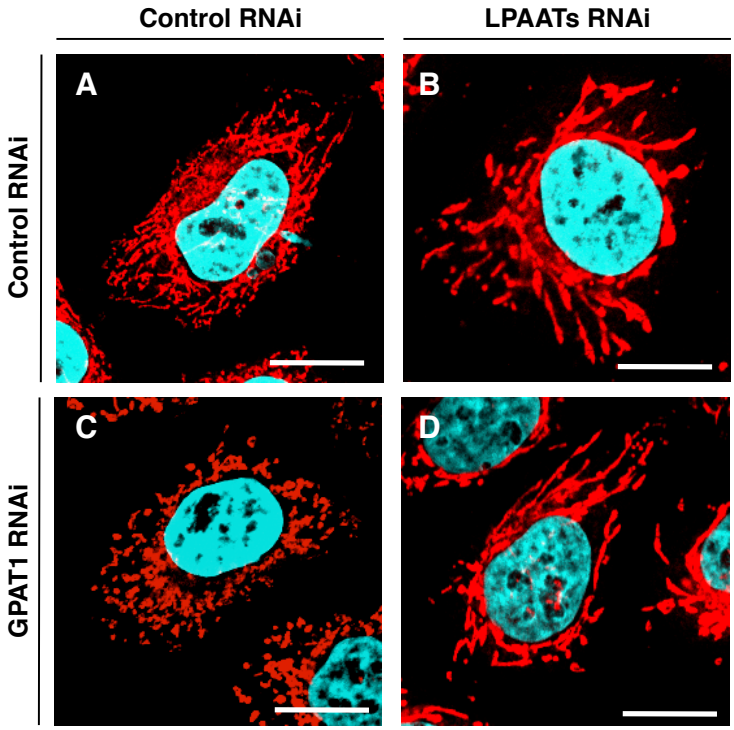

Figure S11

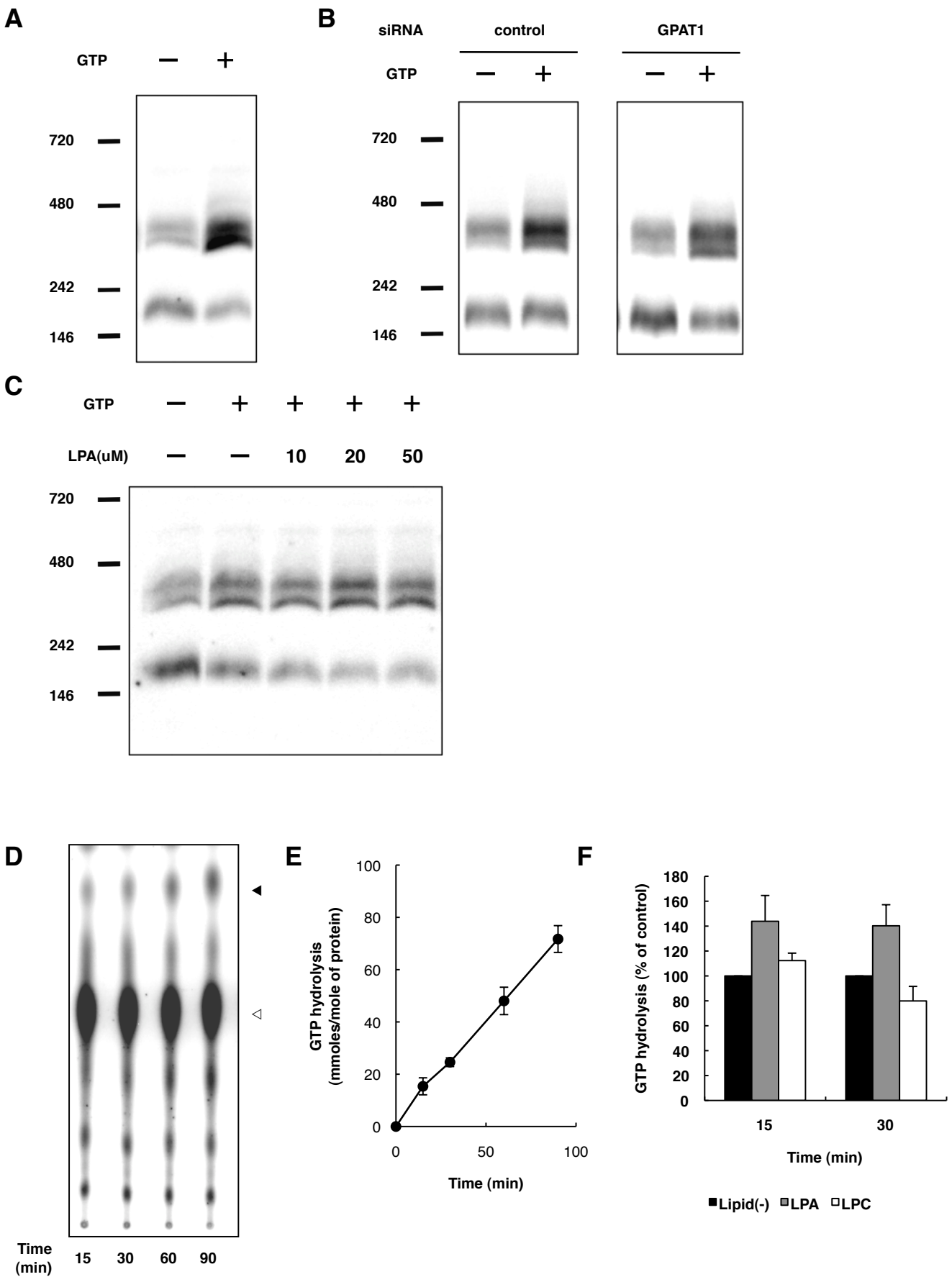
A
GTP
720
480
242
146
B
siRNA
control
GPAT1
GTP
720
480
242
146
C
GTP
LPA(uM)
720
480
242
146
D
Time (min)
15
30
60
90
E
GTP hydrolysis (mmoles/mole of protein)
Time (min)
F
GTP hydrolysis (% of control)
Time (min)
Lipid(-)
LPA
LPC

Supplementary Figure legends

Figure S1

Alignment of ER-GPAT (microsomal GPAT), Mt-GPAT (mitochondrial GPAT), and LPAAT

(A) Alignment of *C. elegans* ER-GPATs (ACL-4 and ACL-5) and their homologues from human and mouse.

(B) Alignment of *C. elegans* Mt-GPAT (ACL-6) and its homologue from human and mouse.

(C) Alignment of *C. elegans* LPAATs (ACL-1 and ACL-2) and their homologues from human and mouse.

Identical amino acids are shown on a black background and similar amino acids are shown on a grey background. Lysophospholipid acyltransferase motifs conserved in AGPAT family members are underlined.

Figure S2

Subcellular localization of *C. elegans* ACL-4, ACL-5 and ACL-6

(A-R) Myc-ACL4 (A-C, J-L), Myc-ACL5 (D-F, M-O) or ACL-6-Myc (G-I, P-R) was expressed in COS-7 cells. The transfected cells were counterstained with antibodies against Myc and calnexin (A-I). Mitochondria were stained with MitoTracker (J-R). White boxes indicate regions enlarged in insets. Scale bars, 10 μm.

(S-U) Transgenic worms expressing ACL-6::GFP translational fusion protein in body wall muscles cells using a *myo-3* promoter. ACL-6::GFP colocalized with MitoTracker in body wall muscle cells. Scale bars, 5 μm.

Figure S3

Mt-GPAT deficiency causes mitochondrial fragmentation in *C. elegans* body wall muscle cells

(A, B) Wild-type (A) or Mt-GPAT (*acl-6*) mutants (B) expressing mitoGFP in body wall muscle cells (*ccIs4251*) were stained with MitoTracker. Body wall muscle cells are outlined with lines. Scale bars, 10 μm. An arrowhead shows the mitochondria, which aren't stained by MitoTracker.

Figure S4

Mt-GPAT mutants show defects in muscle function.

Thrashing upon immersion in liquid (M9) were assessed in wild type and Mt-GPAT (*acl-6)* mutants. Each bar represents the mean ± SEM of 20 trials. ***p<0.001 (Student's t test).

Figure S5

Mt-GPAT functions cell-autonomously to maintain mitochondrial morphology

(A-C) Mt-GPAT (*acl-6*) mutants expressing ACL-6 in the intestinal cells (*ges-1* promoter, A) or body wall muscle cells (*myo-3* promoter, B) were stained with MitoTracker. Body wall muscle cells are outlined with lines. Scale bars, 10 μm. The bar graph shows the relative frequencies of worms with fragmented, partially fragmented or tubular mitochondria in each strain. The experiment was repeated three times (n>20 for each experiment). Bars, mean± SEM. (C).

(D-G) MitoTracker staining of germ cells in wild-type (D), Mt-GPAT (*acl-6*) mutant (E) and *acl-6* mutant expressing ACL-6 in the intestinal cells (*ges-1* promoter, F) or body wall muscle cells (*myo-3* promoter, G). Scale bars, 10 μm.

(H) The percentage of the sterile worms in each strain. Each bar represents the mean ± SEM of at least three independent experiments (n>50 for each experiment).

(I, J) Photographs of *rrf-1* mutants subjected to mock (I) or *acl-6* RNAi (J). Scale bars, 1 mm.

(K) The percentage of sterile worms in *rrf-1* mutants under the each RNAi condition. Each bar represents the mean ± SEM of at least three independent experiments (n>50 for each experiment).

Figure S6

LPA analogues don't inhibit LPAAT activity

(A) LPA acyltransferase activity in the membrane fractions of wild-type worms. 1-oleoyl lysophosphatidic acid (40 μM), [^{14}C]oleoyl-CoA (12.5 μM) and each LPA analogue (20 μM) were used. Each bar represents the mean ± SEM of at least three independent experiments.

(B-E) Structures of LPA and metabolically stabilized LPA analogues

(B) 1-palmitoyl lysophosphatidic acid.

(C) (2R)-1-oleoyl-2-*O*-methyl-glycerophosphothionate (OMPT).

(D) (3S)-1-fluoro-3-hydroxy-4-(linoleoyloxy)butyl-1- phosphonate (XY-26).

(E) 1-palmitoyl alkyl LPA (XY-47).

Figure S7

Mitochondrial fragmentation in *fzo-1* mutants is suppressed by inhibition of *drp-1*

(A-D) MitoTracker staining of body wall muscle cells (A and B) and germ cells (C and D) in *fzo-1* mutants subjected to mock or *drp-1* RNAi. Body wall muscle cells are outlined with lines. Scale bars, 10 μm.

(E) The bar graph shows the relative frequencies of worms with fragmented, partially

fragmented or tubular mitochondria in body wall muscle cells of *fzo-1* mutants or *fzo-1: acl-1* double mutants (n>20).

Figure S8

Inhibition of *drp-1* don't rescue the fertility defects of Mt-GPAT mutants.

The percentage of the sterile worms of Mt-GPAT (*acl-6*) mutants subjected to mock or *drp-1* RNAi. Each bar represents the mean ± SEM of at least three independent experiments. The P value was determined by Student's t test.

Figure S9

Knockdown of Mt-GPAT does not affect mitochondrial protein levels and mitochondrial function in HeLa cells

(A) Real time PCR analysis of Mt-GPATs (GPAT1 and GPAT2) mRNA expression in HeLa cells. The relative expression of Mt-GPATs was normalized by GAPDH mRNA level. Each bar represents the mean ± SEM of at least three independent experiments.

(B) Real time PCR analysis of GPAT1 mRNA expression in HeLa cells treated with control or GPAT1 siRNA. Each bar represents the mean ± SEM of at least three independent experiments.

(C) HeLa cells were transfected with control or GPAT1 siRNA. These cells were stained with 100 nM TMRE and analyzed by FACS. Each bar represents the mean ± SEM of at least three independent experiments.

(D) Assessment of mitochondrial DNA (mtDNA) and nuclear DNA (nDNA) by quantitative real time PCR. Each bar represents the mean ± SEM of at least three independent experiments.

(E) Expression levels of mitochondrial proteins in HeLa cells treated with control or GPAT1 siRNA were evaluated by immunoblotting. Anti-Mfn1 antibody (3C9, Abnova) recognizes both Mfn1 (**) and Mfn2 (*).

Figure S10

Mitochondrial fragmentation in GPAT1-depleted HeLa cells is suppressed by LPAAT depletion

(A-D) HeLa cells were treated with siRNA against the indicated genes and stained with MitoTracker and DAPI. Scale bars, 10 μm.

Figure S11

***In vitro* GTPase activity of Mfn1 is slightly elevated by LPA supplementation**

(A-C) Mfn complexes were analyzed by Blue-native PAGE (BN-PAGE).

(A) Isolated mitochondria of HeLa cells were incubated at 30 °C for 30 minutes in the absence or presence of 400 μM GTP and subjected to BN-PAGE. The separated protein complexes were analyzed by immunoblotting using anti-Mfn1 antibody.

(B) HeLa cells treated with control or GPAT1 siRNA were used. Isolated mitochondria of HeLa cells were incubated at 30 °C for 30 minutes in the absence or presence of 400 μM GTP. The methods of BN-PAGE and immunoblotting were same as (A).

(C) Isolated mitochondria of HeLa cells were incubated at 30 °C for 30 minutes in the absence or presence of 400 μM GTP. Several amount of LPA were added to the mixture. The methods of BN-PAGE and immunoblotting were same as (A).

(D-F) His-tagged Mfn1 recombinant protein was incubated with [α-^{32}P]GTP at 37°C for the indicated times in the absence (D-F) or presence (F) of each lipid (40 μM), and analyzed by

thin layer chromatography followed by digital autoradiography as described. The positions of GDP and GTP are shown by filled arrowhead and open arrowhead, respectively (D). GDP radioactivity was quantified using an image analyzer (E). Mfn1 GTPase activities of lipid containing conditions are expressed as percentages of control activity (F). The values represent the mean ± SEM of three independent experiments.

Table S1

Phenotypic summary of GPATs and LPAATs mutants

(A)

Parental strain	Emb (%) in progeny	
	Mock	*acl-6* RNAi
acl-4(xh10) acl-5(xh19); acl-6(tm3396)/unc-46(e177) dpy-1(e224)	16.5 (n=321)	90.8 (n=131)
acl-4(xh10) acl-5(xh19); acl-6(tm3452)/unc-46(e177) dpy-1(e224)	22.4 (n=178)	58.1 (n=198)

Note: Some of Mt-GPAT and ER-GPAT double mutants (*acl-4 acl-5;acl-6 triple mutants)* born of *acl-4 acl-5;acl-6*/+ parental animals are rescued from embryonic lethality by a maternal contribution of ACL-6. *acl-4 acl-5;acl-6*/+ parental animals subjected to *acl-6* RNAi produce no viable *acl-4 acl-5;acl-6* triple mutants.

(B)

Parental strain	Mock		*acl-1* RNAi	
	Emb (%) in progeny	Larval arrest (%) In progeny	Emb (%) in progeny	Larval arrest (%) In progeny
acl-2(tm3246)	0	0	1 (n=201)	6 (n=199)
acl-2(tm3246); acl-1 (tm3289)/+	0	25.5 (n=649)	25.4 (n=153)	22.8 (n=14)

Note: *acl-2;acl-1* double mutants born of *acl-2;acl-1*/+ parental animals are rescued from embryonic lethality by a maternal contribution of ACL-1. *acl-2;acl-1*/+ parental animals subjected to *acl-1* RNAi produce *acl-2;acl-1* double mutants that show embryonic lethality.

Table S3

Phospholipid composition of Mt-GPAT mutants and GPAT1-depleted HeLa cells

(A) *C. elegans*

	Percent of total phospholipid	
	Wild-type	*acl-6(tm3396)*
Cardiolipin	1.88±0.18	1.78±0.22
Phospahtidic acid	2.94±0.48	2.79±0.21

(B) HeLa cells

	Percent of total phospholipid	
	Control RNAi	GPAT1 RNAi
Cardiolipin	1.94±0.26	2.10±0.19
Phospahtidic acid	3.10±0.13	3.51±0.18

Each data represents the mean ± SEM of three independent experiments.

Supplementary Material and methods

Manipulation of *C. elegans*

Worm cultures, genetic crosses, and other *C. elegans* methods were performed according to standard protocols (Brenner, 1974) except where otherwise indicated. The mutant alleles *acl-1(tm3289)*, *acl-2(tm3246)*, *acl-4(xh10)*, *acl-5(xh19)*, *acl-6(tm3396)* and *acl-6(tm3452)* were isolated in this study by PCR-based screening of TMP/UV-mutagenized libraries (Gengyo-Ando and Mitani, 2000). The primers for *acl-1* deletion screen were: 5'-TCT AGG CCA TCT CAA GTG TC-3'; 5'-GTC GAT TTA CGA GGA GGC AT-3'; 5'-CAA TCT CGT GGA GCG TGG TG-3'; 5'-TTC TGG GTA GAT CCA CAC CT-3'; the primers for *acl-2* deletion screen were: 5'-TTG TAC CCG TTT GTG GCT TA-3'; 5'-CCC ATC ACT CAC TCA TCA TG-3'; 5'-ACC GGG CGC CGA ACT TTA CA-3'; 5'-GGG TGG AGT CAA CAG ACC AC-3'; the primers for *acl-4* deletion screen were: 5'- CTA TTT TCA CTG ACA CAT TCC G-3'; 5'-ACC AAA TCG AAA ATA GGA ATA C-3'; 5'-CCA AGA GTC CTT CGT GTT TC-3'; 5'-GCC CAC GAA GTC ATC ATT CTC-3'; the primers for *acl-5* deletion screen were: 5'-CGA TTT TGT GCT GTG GAC AG-3'; 5'-CTC TCT TCA ATG CTC CAT CC-3'; 5'-GAG TGT CAC AAG CTT ACT CG-3'; 5'-AAT GTT GCC GTT TCT TCG GC-3'; and the primers for *acl-6* deletion screen were: 5'-GTA CTC ATG GTC AAT TCC GC-3'; 5'-ACG TCT CCA CCT TCG GCG AT-3'; 5'-GAT CCT TCC AGA AAG CCG AG-3'; 5'-CGA TAC GAT TGT CAG AGC TG-3'. The following mutations and transgenes were used: *rrf-1(pk1417), fzo-1(tm1133), unc-46(e177) dpy-11(e224)* and *ccIs4251*. Some of the strains used in this work were obtained from *Caenorhabditis* Genetics Center, University of Minnesota, Minneapolis, MN. All mutations and were backcrossed at least five times before further analysis.

Constructs and transgenic worms

DNA injection into the *C. elegans* germ line was carried out as described (Mello *et al*, 1991). The extrachromosomal arrays *xhEx3229 [acl-6p::acl-6 cDNA::GFP, Pser-2::mRFP]*, *xhEx3242 [myo-3p::acl-6 cDNA::GFP, rol-6 (su1006)]*, *xhEx3228 [ges-1p::acl-6 cDNA::GFP, rol-6 (su1006)]*, *xhEx3236 [myo-3p::fzo-1 cDNA::GFP, rol-6 (su1006)]*, *xhEx3258 [myo-3p::hgpat1(WT)::GFP, rol-6 (su1006)]* and *xhEx3259 [myo-3p::hgpat1(R318A)::GFP, rol-6 (su1006)]* were used in this study. The plasmids pTS2 (*acl-6p::acl-6 cDNA::GFP*), pTS3 (*myo-3p::acl-6 cDNA::GFP*), pTS4 (*ges-1p::acl-6 cDNA::EGFP*), pTS5 (*myo-3p::fzo-1 cDNA::GFP*), pYO1 *(myo-3p::hgpat1(WT)::GFP)* and pYO2 *(myo-3p::hgpat1(R318A)::GFP)* were prepared as follows. **pTS2:** a genomic fragment including 3.2kb upstream of the *acl-6* initiation codon was PCR amplified using the primers 5'-AAG AGC TGC AGT TTT ATC AAT AAG CAT TTA ATC-3' and 5'-TCT AGA CCG TCT TCT GAA CGA ATG CTC C-3', and cloned into pPD95.67 (NLS-) at the *Pst*I and *Xba*I sites. The full length of *acl-6* cDNA was PCR amplified using the primers 5'-TCT AGA ATG GAG CTC GAC GTG GAA TC-3' and 5'-CCC GGG CTT TGA CTT CCA AAA CTC GTT C-3' and cloned downstream of *acl-6* promoter at the *Xba*I and *Sma*I sites. **pTS3**: Firstly, pPD95.77 was modified by inserting *Sac*I and *Not*I sites between the *Sma*I and *Bal*I sites. *myo-3* promoter derived from *Pmyo-3::fat-3* (a gift from Giovanni M. Lesa) was replaced with *unc-122* promoter of pPD95.77 using the *Hind*III and *BamH*I sites to yield *Pmyo-3::GFP* vector. *acl-6* cDNA was PCR amplified using the primers 5'-AGG TCG ACT CTA GAA TGG AGC TCG ACG TGG AAT C-3', and 5'-CCT TTG GCC GCG GCC GCG CTT TGA CTT CCA AAA CTC GTT-3', and cloned into the *Pmyo-3::GFP* vector at the *Xba*I and *Not*I sites. **pTS4**: *ges-1* promoter region was ligated into pFX_EGFPT

(Gengyo-Ando *et al,* 2006) using the TA cloning strategy to fuse the coding sequence region of EGFP. *acl-6* cDNA was PCR amplified using the primers 5'-GCG GCC GCA TGG AGC TCG ACG TGG AAT C-3' and 5'-GCG GCC GCC TTT GAC TTC CAA AAC TCG TTC-3' and cloned using the *Not*I site. **pTS5:** pTS5 was constructed in a similar manner to pTS3 using the primers 5'-ATA TAT CTA GAA TGT CTG GCA CAG CAA GCT TAG-3', and 5'-CAC AGT GTG CGG CCG CGC TGG CGT TGG CGG AGA GTC CG-3'. **pYO1:** pYO1 was constructed in a similar manner to pTS3 using the primers 5'-GCA GAG CTC ATG GAT GAA TCT GCA CTG ACC-3', and 5'-GCA TAA GGG CGG CCG CAT CAG CAC CAC AAA ACT CAG-3'. GPAT1(WT)-FLAG vector was used as a template. **pYO2:** pYO2 was constructed was constructed in a similar manner to pYO1. GPAT1(R318A)-FLAG vector was used as a template.

Phenotypic analysis of *acl* mutants

Viability analysis: adult worms were allowed to lay eggs for 2-3h. Unhatched eggs were examined 24 h after being laid, and larvae that failed to reach the L4 stage by day 3 post-hatch were scored as larval arrest. To confirm that depletion of all *C. elegans* GPAT results in lethality, *acl-6(tm3396* or *tm3452)/unc-46(e177) dpy-11(e224)*; *acl-4 acl-5* mutants were subjected to *acl-6* RNAi to eliminate maternally-derived *acl-6* mRNA and were scored for embryonic lethality (see Supplementary Table S1A). In a similar manner, *acl-2(tm3246); acl-1(tm3289)*/+ mutants were subjected to *acl-1* RNAi and were scored for embryonic lethality and larval arrest (see Supplementary Table S1B).

Sterility analysis: L1 animals were cloned to individual plates and were scored for the presence or absence of progeny. To determine brood size, at least 10 L4 worms were individually plated, allowed to develop into adults, and then the number of eggs laid and the

number of progeny that hatched were counted. To visualize nuclear morphology of germ cells, gonads were dissected, fixed, and stained with DAPI as described previously (Rose *et al,* 1997). Adult hermaphrodites were cut open, fixed in 3% paraformaldehyde in PBS for 2 hours at room temperature. Following fixation, gonads were washed once in M9 buffer and post- fixed in -20 °C methanol for 5 minutes and stained with 0.4 mg/ml DAPI in M9.

Thrashing assay: Young adult hermaphrodites were placed in drops of PBS, and simple rhythmic thrashing swimming was measured. Swimming was scored as the number of seconds taken for 30 thrashes and calculated backward to the swimming rate. Each worm was scored twice.

RNAi procedure in *C. elegans*

Feeding RNAi: Feeding RNAi was carried out as described previously (Kamath *et al,* 2001). Feeding RNAi clones were obtained from the Ahringer library (Kamath *et al,* 2003) or from the ORFeome RNAi collection (Rual *et al,* 2004).

Injection RNAi: *acl-6* dsRNA was prepared by *in vitro* transcription with T7 polymerase using PCR product as a template (Promega). The template was amplified by PCR from pTS2 using primers: forward, 5'-TAA TAC GAC TCA CTA TAG GAT GGA GCT CGA CGT GGA ATC-3'; reverse, 5'-TAA TAC GAC TCA CTA TAG GCC AAA ACT CGT TCC AGA TTG-3'. dsRNA was microinjected into the syncytial gonad of *rrf-1(pk1417)* adult hermaphrodites at final concentrations of 1 μg/μL. Injected worms were allowed to recover at 20 °C for 24 hours post-injection, were replica plated and allowed to lay eggs for 8 hours. Their progeny were cloned to individual plates and incubated for 3 days at 20 °C. Then they were scored for the presence or absence of progeny.

Cell culture and transfection

COS-7, HEK293 and HeLa cells were maintained in DMEM supplemented with 10% fetal calf serum and 100 units/mL penicillin, 100 mg/mL streptomycin, 2 mM L-glutamine. Transfection was performed using Lipofectamine 2000 (Invitrogen) according to the manufacturer's instruction. To examine subcellular localization of *acl* genes, full length cDNA of each *acl* gene (*acl-4, acl-5,* or *acl-6*) was cloned into pcDNA3 vector (Invitrogen) and was transfected into COS-7 cells. Expression vectors were prepared as follows. Full-length cDNAs for *acl-6* were amplified by PCR from *C. elegans* cDNA and were cloned into pcDNA3-Myc vector (C-terminal Myc vector) at the *Hin*dIII and *Xho*I site. Full-length cDNAs for *acl-4* and *acl-5* were amplified by PCR and cloned into Myc-pcDNA3 vector (N-terminal Myc vector) at the *Not*I *and Apa*I sites. The primers used for amplification were as follows: *acl-4*, 5'-CGA AAA ACG CGG CCG CTG ATG CTG GGA ATC GAG CAC CTG CTG TTT GTG TTA AC-3' and 5'-TGG GGG GGC CCT CAA GTT TTC ACC AAA GAA AC-3'; *acl-5*, 5'-ATA AGA ATG CGG CCG CTG ATG ATC TTC CTG GTG TTT TGG TTT CTG ATT TTA-3' and 5'-AAA ATG GGC CCT TAG TCA GAC TTA ATG TGC TCG-3'; *acl-6*, 5'-ACT GGC GGA AGC TTA TGG AAC TGG ACG TGG AAT CCA CCA GC-3' and 5'-GAA TAG GGC TCG AGT TTG ACT TCC AAA ACT CGT TCC-3'. These primers were designed based on the codon-usage preference in mammalian cells. For GPAT assay, full length cDNAs of human GPAT1 was cloned into pcDNA3 vector, and was transfected into HEK293 cells. Expression vectors were prepared as follows. Full-length cDNAs for GPAT1 were amplified by PCR from HeLa cDNA and were cloned into pcDNA3-FLAG vector (C-terminal FLAG vector) at the *EcoRI* and *Xho*I site. The primers used for amplification were as follows: GPAT1, 5'-ATG CAT GCG AAT TCA TGG ATG AAT CTG CAC TGA C-3' and 5'-GCC TCG AGC CAG CAC CAC AAA ACT CAG AA-3'.

GPAT1(R318A) were constructed by site-directed mutagenesis. The expression level of protein was analyzed by immunoblotting using anti-FLAG (1:4000, 1E6, Wako) antibody.

RNAi in HeLa cells

siRNA against GPAT1 (siRNA 1: CAA UCA AAA GCC GUU AAC A, siRNA 2: GCU UCA GGC AAU AAU CUC A, obtained from Nippon EGT (Toyama, Japan)), Mfn1 (AAA CUU AUC AAU CCA GCU AUC CAG C, purchased from Invitrogen), Mfn2 (AAU CCC AGA GGG CAG AAC UUU GUC C, purchased from Invitrogen), Drp1 (ACU AUU GAA GGA ACU GCA AAA UAU AAG, obtained from Hokkaido System Science (Sapporo, Japan)), LPAAT1 (GCU GGA CCC UUC UAA UUC A, obtained from Nippon EGT (Toyama, Japan)) and LPAAT2 (combination of 4 siRNAs; 1: GUG CGA AGC UUC AAG UAC U, 2: GCC GGA CGG UGG AGA ACA U, 3: CGG CCG AGU UCU ACG CCA A, 4: GCG CUG UGC UUC ACG GUG U, purchased from Dharmacon) were introduced to HeLa cells using Lipofectamine 2000 according to the manufacturer's instruction. Control siRNA (*Silencer* Negative Control #1 siRNA) was obtained from Ambion. For analyzing protein expression, HeLa cells were lysed with lysis buffer (20 mM Tris-HCl (pH 7.4), 1% Triton X-100, 0.5% NP-40, 5 mM EDTA) containing a protease inhibitor mixture. The lysates were cleared by centrifugation at 12, 000 g for 20 minutes. Then the supernatant fractions were analyzed by immunoblotting using monoclonal anti-Mfn1 (1:1000, 3C9, Abnova), anti-Mfn2 (1:1000, 4H8, Abnova), anti-Opa1 (1:1000, BD Transduction Laboratories), anti-Drp1 (1:1000, BD Transduction Laboratories), anti-Bax (1:500, BD Pharmingen), anti-Bak (1:500, BD Pharmingen), anti-Bcl-x (1:250, BD Pharmingen), polyclonal anti-MIB (1:1000, Eura *et al,* 2006), anti-Tom70 (1:1000, Suzuki *et al,* 2002) and anti-Tim17 (1:1000, Ishihara and Mihara 1998) antibodies.

Immunocytochemistry

Cells grown on poly-L-lysine-coated glass coverslips were fixed with 3.7% formaldehyde and permeabilized with 0.5% Triton X-100 (vol/vol). Cells were then incubated with mouse monoclonal anti-Myc antibody (1:1000, 9E10, Sigma) or rabbit anti-calnexin N-terminal polyclonal antibody (1:1000, StressGen Biotechnologies Corp., Victoria, Canada), and visualized with Alexa Fluor 488 goat anti-mouse IgG (H + L) or Alexa Fluor 594 goat anti-rabbit IgG (H + L) (1:2000, Invitrogen). 4', 6-diamidino-2-phenylindole (DAPI, Sigma) in PBS was used to stain nuclei. The samples were analyzed with a confocal fluorescence microscope (LSM510, Carl Zeiss Inc., Thornwood, NY).

FACS Analysis

HeLa cells were stained with 100 nM tetramethylrhodamine ethyl ester perchlorate (TMRE, Molecular Probes) in DMEM for 30 minutes. Then cells were trypsin-harvested, resuspended in PBS and analyzed by a FACS Calibur analyzer (BD).

Quantitative real-time PCR

Total RNA from cells was extracted using Isogen (Nippongene, Toyama, Japan) and reverse-transcribed using the High Capacityc DNA Reverse Transcription kit (Applied Biosystems, Foster City, CA). Genomic DNA from cells was extracted by QIAamp DNA mini kit (Qiagen) according to the manufacturer's instructions. Quantitative real-time PCR was performed using SYBR_ Green PCR Master Mix (TaKaRa) and Light-Cycler 480 (Roche Diagnostics). The sequences of the oligonucleotides were as follows; GPAT1, 5'-AGC CTG TGC TAC CTT CTC TCC-3' and 5'-TCC TGG TCA TCG TGC TCT G-3'; GPAT2, 5'-GGA AGT ATC GCC CCT TTG TG-3' and 5'-CCC GAA ACC TTG TGT TCT

CC-3'; GAPDH 5'-GCC AAG GTC ATC CAT GAC AAC T-3' and 5'-GAG GGG CCA TCC ACA GTC TT-3'. The transcript number of human GAPDH was quantified, and each sample was normalized on the basis of GAPDH content. The primer sets for the amplification of mtDNA (65 bp) and β2M coding nuclear (95 bp) fragments were used as described previously (Malik *et al*, 2011).

BN-PAGE

Mfn complex formation and BN-PAGE were performed as previously (Ishihara *et al*, 2004), except that NativePAGE™ Novex® 4-16% Bis-Tris Gel (Invitrogen), Native Mark™ Unstained Protein Standard (Invitrogen) and anti-Mfn1 antibody (3C9, Abnova) were used.

Purification of recombinant Mfn1 proteins and assay for GTPase activities

Recombinant Mfn1 purification and measurement of GTP hydrolysis were performed as previously (Ishihara *et al*, 2004).

Supplementary References

Brenner S (1974) The genetics of *Caenorhabditis elegans*. *Genetics* **77:** 71–94

Gengyo-Ando K, Mitani S (2000) Characterization of mutations induced by ethyl methanesulfonate, UV, and trimethylpsoralen in the nematode *Caenorhabditis elegans*. *Biochem Biophys Res Commun* **269:** 64–69

Gengyo-Ando K, Yoshina S, Inoue H, Mitani S (2006) An efficient transgenic system by TA cloning vectors and RNAi for *C. elegans*. *Biochem Biophys Res Commun* **349:** 1345–1350

Ishihara N, Mihara K (1998) Identification of the protein import components of the rat mitochondrial inner membrane, rTIM17, rTIM23, and rTIM44. *J Biochem* **123:** 722-732

Kamath RS, Martinez-Campos M, Zipperlen P, Fraser AG, Ahringer J (2001) Effectiveness of specific RNA-mediated interference through ingested double-stranded RNA in *Caenorhabditis elegans*. *Genome Biol* **2:** 1–10

Kamath RS, Fraser AG, Dong Y, Poulin G, Durbin R, Gotta M, Kanapin A, Le Bot N, Moreno S, Sohrmann M, Welchman DP, Zipperlen P, Ahringer J (2003) Systematic functional analysis of the *Caenorhabditis elegans* genome using RNAi. *Nature* **421:** 231–237

Malik AN, Shahni R, Rodriguez-de-Ledesma A, Laftah A, Cunningham P (2011) Mitochondrial DNA as a non-invasive biomarker: accurate quantification using real time

quantitative PCR without co-amplification of pseudogenes and dilution bias. *Biochem Biophys Res Commun* **412:** 1–7

Mello CC, Kramer JM, Stinchcomb D, Ambros V (1991) Efficient gene transfer in *C. elegans*: extrachromosomal maintenance and integration of transforming sequences. *EMBO J* **10:** 3959–3970

Rose KL, Winfrey VP, Hoffman LH, Hall DH, Furuta T, Greenstein D (1997) The POU gene ceh-18 promotes gonadal sheath cell differentiation and function required for meiotic maturation and ovulation in *Caenorhabditis elegans*. *Dev Biol* **192:** 59-77

Rual JF, Ceron J, Koreth J, Hao T, Nicot AS, Hirozane-Kishikawa T, Vandenhaute J, Orkin SH, Hill DE, van den Heuvel S, Vidal M (2004) Toward improving *Caenorhabditis elegans* phenome mapping with an ORFeome-based RNAi library. *Genome Res* **14:** 2162–2168

Suzuki H, Maeda M, Mihara K (2002) Characterization of rat TOM70 as a receptor of the preprotein translocase of the mitochondrial outer membrane. *J Cell Sci* **115:** 1895-1905